



Removal of hydrogen sulfide using carbonated steel slag

Asaoka, Satoshi ; Okamura, Hideo ; Morisawa, Ryosuke ; Murakami, Hiroshi ; Fukushi, Keiichi ; Okajima, Toshihiro ; Katayama, Misaki ;...

(Citation)

Chemical Engineering Journal, 228:843-849

(Issue Date)

2013-07-15

(Resource Type)

journal article

(Version)

Accepted Manuscript

(Rights)

©2013 Elsevier.

This manuscript version is made available under the CC-BY-NC-ND 4.0 license
<http://creativecommons.org/licenses/by-nc-nd/4.0/>

(URL)

<https://hdl.handle.net/20.500.14094/90003338>



Removal of hydrogen sulfide using carbonated steel slag

Satoshi ASAOKA^{a*}, Hideo OKAMURA^a, Ryosuke MORISAWA^b, Hiroshi
MURAKAMI^c, Keiichi FUKUSHI^d, Toshihiro OKAJIMA^e, Misaki
KATAYAMA^f, Yasuhiro INADA^f, Chihiro YOGI^g, Toshiaki OHTA^g

^aResearch Center for Inland Seas, Kobe University, 5-1-1 Fukaeminami,
Higashinada, Kobe, 658-0022 JAPAN

^bFaculty of Maritime Sciences, Kobe University, 5-1-1 Fukaeminami,
Higashinada, Kobe, 658-0022 JAPAN

^cKOBELCO Research Institute INC., 1-5-5 Takatsukadai, Nishi, Kobe,
651-2271 JAPAN

^dGraduate School of Maritime Sciences, Kobe University, 5-1-1 Fukaeminami,
Higashinada, Kobe, 658-0022 JAPAN

^eKyushu Synchrotron Light Research Center, 8-7, Yayoigaoka, Tosu, Saga,
841-0005 JAPAN

^fCollege of Life Science, Department of Applied Chemistry, Ritsumeikan
University, 1-1-1 Nojihigashi Kusatsu, Shiga, 525-8577 JAPAN

^gSR Center, Ritsumeikan University, 1-1-1 Nojihigashi Kusatsu, Shiga,
525-8577 JAPAN

*Corresponding author:

Tel: +81-78-431-6357, Fax: +81-78-431-6272,

E-mail address: s-asaoka@maritime.kobe-u.ac.jp

Address: Research Center for Inland Seas, Kobe University, 5-1-1

Fukaeminami, Higashinada, Kobe, 658-0022 JAPAN

Abstract

High levels of hydrogen sulfide are sometimes observed in the pore water of eutrophic sediments. It is important to reduce the hydrogen sulfide concentration to maintain health ecosystems as well as aquaculture activities in enclosed water bodies. The purpose of this study is to reveal the removal mechanism of hydrogen sulfide using carbonated steel slag produced through carbonation processes to alleviate alkaline impacts. Batch adsorption experiments revealed that hydrogen sulfide was adsorbed onto carbonated steel slag based on a pseudo-first-order kinetic model; its adsorption maximum was 7.5 mg g^{-1} . The removal mechanisms of the hydrogen sulfide included (1) the formation of pyrite, and (2) oxidation to sulfur coupled with the reduction of manganese oxide on the carbonated steel slag.

Key words

adsorption, environmental remediation, manganese oxide, marine sediment, pyrite

1. Introduction

Iron slag, by-product of the steelmaking process, is roughly classified into two categories: blast furnace slag and steel slag. The former is derived from the conversion process of iron ore into pig iron, while the latter is generated from the purification process of pig iron into steel. In Japan, 24.4 and 14.5 Mt of blast furnace slag and steel slag, respectively, are generated annually [1]. The slag has been conventionally reused for roadbed construction material as a coarse aggregate for concrete and as a raw material for cement [1, 2]. Moreover, considering the recent momentum towards promoting a recycling-conscious society, it is practical to explore and test new applications for iron slags. So far, phosphate adsorption and soil aquifer treatment in terms of removal of dissolved organic carbon and several ions using iron slags have been studied [3-5]. For coastal environmental remediation, characterization of blast furnace slag and adsorption test have been conducted. The results show that blast furnace slag could suppress phosphate-releasing flux and decrease the acid volatile sulfide concentration in organically enriched sediments [6]. Field experiments also revealed that steelmaking slag reduced the concentration of hydrogen sulfide in sediments

[7].

On the other hand, a large amount of calcium dissolved into seawater from slags triggers a rapid increase of pH because the slags contain free calcium. Therefore, the seawater pH increases up to 12.3 due to the hydrolysis of calcium hydroxide [8, 9]. With regard to the environment, significant pH increase might have negative impacts on ecosystems. For instance, diatoms show a decreased growth rate at pH over 8.5 [10-12].

As a result, carbonated steel slag was taken into consideration to alleviate significant pH increases. Carbonated steel slag was generally produced by purging CO₂ gas onto the steel slag or piling the slag up in the field to carbonize the surface. Therefore, rapid pH increases were not observed in batch experiments that involved the application of carbonated steel slag for the remediation of sediments [13], because the major calcium species of carbonated steel slag were considered to be calcium or magnesium carbonate [14, 15].

In this study, we focused on the removal of hydrogen sulfide, which is one of the more promising functions of steel slag [16, 17]. Generally, a high level of hydrogen sulfide has been observed in marine sediments accumulated in

enclosed or semi-enclosed water bodies located adjacent to large metropolitan areas [18]. The sediments in these enclosed water bodies are affected by significant terrigenous organic matter loads, and their oxidative decomposition of organic matter consumes dissolved oxygen. Hydrogen sulfide was generated by sulfate reducing bacteria under such anoxic conditions. Hydrogen sulfide has a negative impact on aquaculture activities because it interferes with cytochrome c oxidase, the last enzyme of the electron transport system [19]. As a result, viability of benthic organisms and fishes decreased due to high toxicity [20]. Hydrogen sulfide may also cause blue tides and bad odor when it is upwelling through water column. Therefore it is very important to reduce the hydrogen sulfide concentration in order to maintain healthy ecosystems, aquaculture activities and protect aquatic environments.

The removal of hydrogen sulfide by steelmaking slag (non-carbonated steelmaking slag) is considered to be caused by sulfide mineralization or oxidation [16, 17]. Although the carbonated steel slag is expected to have less severe aquatic environmental impacts compared to non-carbonated slag in terms being less alkaline, there are few studies that address the mechanism

of the removal of hydrogen sulfide to remediate coastal environment. The purpose of this study was to reveal the removal mechanism of hydrogen sulfide by carbonated steel slag and to quantify its removal performance.

2. Materials and methods

2.1 Carbonated steel slag used in this study

The carbonated steel slag 0.8 to 5 mm in diameter used in this study was provided by Kobe Steel, Ltd. It was produced from steel slag derived from converter furnaces. The steel slag was piled up in the field for 2 months so the material's surface would be naturally carbonized.

2.2. Characterization of the carbonated steel slag

The chemical composition of the carbonated steel slag was determined as follows. The concentrations of CaO, SiO₂, MgO, Al₂O₃, P₂O₅ and MnO were determined by X-ray fluorescence (XRF) spectroscopy (Simultix SYS3552, Rigaku). Sulfur was determined with a carbon/sulfur combustion analyzer (EMIA-810, Horiba). Total iron and calcium carbonate were determined by titrimetric methods followed by ISO 2597-2 [21] and JIS R9011, 2006 [22], respectively. The analytical method is also summarized in Table 1.

The concentration of environmentally regulated elements was determined on the basis of the Japanese standard method JIS-K-0058-2 [23]. The analytical method is summarized in Table 2.

The specific surface area was determined by the Brunauer-Emmett-Teller method (nitrogen gas adsorption) using surface area and pore size analyzers (AUTOSORB-1; Quantachrome). A scanning electron microscope (SEM; ESEM-2700; Nikon) with energy dispersive X-ray (EDX) spot analysis was also used to study the morphology.

2.3. Dissolution tests of environmentally regulated substances

Environmentally regulated substances dissolved from the carbonated steel slag were examined using the determination method for soil pollution criteria established by the Ministry of Environment, Japan.

The pH of ultrapure water was adjusted between 5.5 and 6.3 by adding HCl. The slag was added to the ultrapure water to a concentration of 10 w/v% and stirred for 6 h using a magnetic stirrer at a speed of 200 rpm at 20 °C. After stirring, the solution was left undisturbed for 30 min. Thereafter the solution was centrifuged at 3000 rpm for 20 min. The supernatant was filtered through a 0.45- μ m membrane filter (HA, Millipore). The environmentally regulated substances in the filtrate were determined following the standard method [24]. The analytical method is summarized in Table 3.

2.4 Adsorption experiments for hydrogen sulfide

The hydrogen sulfide solution was prepared as follows: Tris-HCl buffer (Kanto Kagaku) was added to 500 mL of pure water deaerated with N₂ gas to

a final concentration of 30 mmol L⁻¹. Thereafter, an aliquot of Na₂S•9H₂O (Wako Pure Chemical Industries) was dissolved in the solution. The concentrations of hydrogen sulfide were 10 and 100 mg L⁻¹, representing the possible range in the pore water of organically enriched sediments. The pH of the solution was adjusted to 8, which is the general seawater pH, by adding HCl.

The batch experiments were conducted in triplicate. 50 mL of the hydrogen sulfide solution was slowly dispensed into a 100 mL vial bottle, and 0.2 g of the carbonated steel slag was added to the solution. Thereafter, the head space of the bottle was replaced with N₂ gas. The bottle was plugged with a rubber cork and sealed with an aluminum cap. It was agitated moderately at 100 rpm at 25 °C in a constant-temperature oven, and the time courses of hydrogen sulfide concentration were measured using a detection tube (200SA or 200SB: Komyo Rikagaku Kougyo). The initial and final pH and Eh of the solution were also measured by a pH electrode (F-53: Horiba) and an ORP electrode (RM-30P:DKK-TOA), respectively.

The carbonated steel slag reacted with 100 mg L⁻¹ of the initial hydrogen sulfide concentration was analyzed as described below.

2.5. X-ray absorption fine structure (XAFS) analyses and data processing

Sulfur K edge XAFS spectra (range: 2440-2540 eV) were measured using BL10 in the SR Center, Ritsumeikan University, Japan. The synchrotron radiation from a bending magnet was monochromatized with a Ge(111)

double-crystal monochromator. XAFS spectra were measured in a partial fluorescence yield (PFY) mode using a SDD detector (Techno X Co. Ltd.) in a He-gas filled atmospheric-pressure chamber or a total electron yield (TEY) mode in a vacuum chamber. The X-ray energies around the K edges of the sulfur were calibrated with the spectra of CuSO_4 obtained using the TEY mode. The K edge main peak of sulfate was set to 2481.6 eV [25].

The XAFS spectra of the relatively flat carbonated steel slag samples mounted on double-stick tape (NW-K15; Nichiban) on a copper sample holder were measured using the PFY mode. The final solution was dispensed into a polyethylene bag (9 μm) and set in a similar manner. The angles between the incident X-ray and the sample surfaces were adjusted at approximately 10 degrees. The standards were measured using the TEY mode.

Manganese K edge XAFS spectra (range 6210-6770 eV) were measured in BL11 at the Kyushu Synchrotron Light Research Center, Japan. The synchrotron radiation was monochromatized with a Si(111) double-crystal monochromator. The sample XAFS spectra were measured using the X-ray fluorescence yield mode with a Lytle detector. Samples were sealed with polypropylene film and were positioned at 45° to the incident beam in the fluorescence mode. The X-ray energy was calibrated by defining the K edge pre-edge peak of d-MnO_2 fixed at 6540 eV. The standards were also measured by the transmission mode using an ionization chamber filled with mixed gases: He 70% and N_2 30% for an incident chamber (I_0 ; 17 cm), and N_2 100% for a transmitted chamber (I ; 31cm).

Iron K edge XAFS spectra (range 7080-7250 eV) were measured in BL3 at the SR Center, Ritsumeikan University, Japan. The synchrotron radiation was monochromatized with a Si(220) double-crystal monochromator. The sample XAFS spectra were measured using the X-ray fluorescence yield mode with a three-element Ge solid state detector, SSD (GUL0110S: Canberra). Samples were sealed with polypropylene film and were positioned at 45° to the incident beam in the fluorescence mode. The X-ray energy was calibrated by defining the K edge pre-edge peak of hematite fixed at 7112 eV. The standards were also measured in the transmission mode using an ionization chamber filled with mixed gases: Ar 15% and N₂ 85% for the incident chamber (I₀; 4.5 cm) and Ar 50% and N₂ 50% for the transmitted chamber (I; 31 cm).

The spectra obtained by XAFS analyses were processed using XAFS spectra processing software (REX2000 ver. 2.5: Rigaku co. Ltd.). The absorption edge (E₀) was defined as the local maximal value in the spectrum.

An Eh–pH diagram of manganese in the presence of sulfur was illustrated by the geochemical modeling software, Geochemist's Workbench 9.0 (RockWare). The parameters used in this thermodynamic calculation were as follows: the activities were referred to liquid phase concentration and set to be 2.7 μmol L⁻¹ for Mn²⁺ and 3 mmol L⁻¹ for SO₄²⁻. The pressure and temperature were set at 1.013 hPa and 25 °C, respectively. The manganese concentrations in the liquid phases were measured by graphite furnace atomic absorption spectrometry (Z8270: Hitachi) after being filtrated

through a 0.2- μm hydrophilic PVDF filter (MILLEX: Millipore) and diluted 50 times using 2% analytical grade HNO_3 .

3. Results and discussion

3.1. Characterization of the carbonated steel slag

The chemical composition of the carbonated steel slag used in this study included mainly calcium carbonate, iron compounds and calcium oxide, etc. (Table 1). Approximately 47% of the calcium in the carbonated steel slag was carbonated.

The concentrations of environmentally regulated substances in the carbonated steel slag were lower than those set by the Japanese environmental criteria (Table 2). The amounts of environmentally regulated substances dissolved from the carbonated steel slag were also obviously low compared to the Japanese environmental criteria (Table 3).

The SEM images of the small particles in the carbonated steel slag and the chemical compositions obtained by the semi quantitative mode with EDX are shown in Fig. 1 and Table 4, respectively. These small particles were mainly composed of magnesium, calcium, carbonate, silicate, aluminate and iron. Sodium, titanium, manganese, copper and zinc were non-homogenously distributed in the particles.

The specific surface area of the carbonated steel slag used in this study was $14.4 \text{ m}^2 \text{ g}^{-1}$. The specific surface areas of steel slag reported in previous studies were 0.822-1.850, 2.09 and $5.74 \text{ m}^2 \text{ g}^{-1}$ [26-28]. The slag used in this

study has a large specific surface area compared to general steel slags.

3.2 Adsorption of hydrogen sulfide onto the carbonated steel slag

The adsorption kinetics of hydrogen sulfide onto the carbonated steel slag are shown in Fig 2. In the case with an initial concentration of 10 mg L⁻¹, the hydrogen sulfide was removed in 12 h. However, when the initial concentration was 100 mg L⁻¹, the concentration of hydrogen sulfide reached equilibrium at 9 h, and the color of the hydrogen sulfide solution with the carbonated steel slag turned yellow. The amount of hydrogen sulfide adsorbed by the carbonated steel slag was 7.5 mg g⁻¹. The concentration of the hydrogen sulfide in eutrophic marine sediment pore water ranged from 0.1-75 mg L⁻¹ [18] (Asaoka, unpublished), fitting within concentration ranges obtained in this experiment. Hence, the adsorption maximum of the hydrogen sulfide onto the carbonated steel slag in eutrophic marine sediment pore water was estimated to be at the same level. The adsorption maximum was lower than that of other recycled industrial materials, 108 mg g⁻¹ for granulated coal ash [29], 37.5 mg g⁻¹ for noncarbonated steel slag [17] and 12 mg g⁻¹ for crushed oyster shells [30].

In order to estimate the rate constant for the hydrogen sulfide removal, the adsorption kinetics of hydrogen sulfide onto the carbonated steel slag were fit by the pseudo-first-order equation (1; [31]), the pseudo-second-order equation (2; [32]), and the intraparticle diffusion model equation (3; [33]).

$$\log(q_e - q_t) = \log q_e - \frac{K_1}{2.303}t \cdot \cdot \cdot (1)$$

$$\frac{t}{q_t} = \frac{1}{K_2} + \frac{1}{q_e}t \cdot \cdot \cdot (2)$$

$$q_t = K_i t^{\frac{1}{2}} \cdot \cdot \cdot (3)$$

where q_e and q_t are the amounts of hydrogen sulfide adsorbed per gram of carbonated steel slag (mg g^{-1}) at equilibrium and time t , respectively. K_1 , K_2 , K_i , and t are the pseudo-first-order rate constant (h^{-1}), the pseudo-second-order rate constant ($\text{g mg}^{-1} \text{ h}^{-1}$), the intraparticle-diffusion rate constant ($\text{mg g}^{-1} \text{ h}^{-1/2}$), and time (h), respectively.

The adsorption kinetics of hydrogen sulfide onto the carbonated steel slag was fitted well by the pseudo-first-order equation and the intraparticle diffusion equation. The correlation coefficient for the linear regression of each kinetic equation is shown in Table 5. In the case with the initial concentration of 100 mg L^{-1} , the correlation coefficient of the intraparticle diffusion equation was quite similar to that of the pseudo-first-order equation. However, the correlation coefficient of the initial concentration of 10 mg L^{-1} was not fit well by the intraparticle diffusion equation. On the other hand, the pseudo-first-order equation could fit both initial concentrations of 10 and 100 mg L^{-1} . Therefore, the pseudo-first-order

equation was suitable for expressing the adsorption kinetics of hydrogen sulfide onto the carbonated steel slag (Fig. 3). The pseudo-first-order rate constants obtained in this study were 0.11 and 0.16 h⁻¹ for the hydrogen sulfide initial concentrations of 10 mg L⁻¹ and 100 mg L⁻¹, respectively.

3.3. Revealing the adsorption mechanism of hydrogen sulfide onto the carbonated steel slag using XAFS

The sulfur K edge XANES spectra of the carbonated steel slag after adsorption of hydrogen sulfide (final slag) and of the yellow-colored hydrogen sulfide solution, along with the standards of pyrite and sulfur, are shown in Fig. 4. The sulfur K edge XANES spectrum of the carbonated steel slag without hydrogen sulfide adsorption (initial slag) is not shown in Fig. 4 because it did not have significant peaks. On the other hand, new peaks at around 2472 eV were observed in the final slag and the yellow-colored solution. The dotted lines in Fig. 4 are curve-fitting results using standard spectra. The sulfur K edge XANES spectra of the final slag could be fitted by a combination of 24.3% sulfur and 75.7% pyrite. The spectra of the yellow-colored solution corresponded well with sulfur. Sulfur in the liquid phase might be derived from the sulfur that was oxidized from hydrogen sulfide on the surface of the carbonated steel slag.

Previous reports revealed that iron and manganese played important roles in removing hydrogen sulfide [17, 34]. Therefore, we next focused on the redox reactions related to iron and manganese in the carbonated steel slag.

The iron K edge XANES spectra of the initial and final slags, several iron standards, and the curve-fitting results are shown in Fig. 5. The iron K edge XANES spectra of the initial slag could be fitted by the combination of 7.2% $\text{Fe}(\text{OH})_2$, 69.4% FeO and 23.4% $\text{FeO}(\text{OH})$. On the other hand, the final slag could be fitted by the combination of 10.5% $\text{Fe}(\text{OH})_2$, 54.5% FeO , 29.5% $\text{FeO}(\text{OH})$ and 5.6% FeS_2 , indicating that pyrite (FeS_2) was newly formed on the surface of the final slag.

The manganese in the carbonated steel slag could not be identified because both the initial and final slag XANES spectra could not be fitted by the manganese standards (Fig. 6). However, the manganese K edge peak of the initial slag had a peak at 6553.4 eV, while a new shoulder peak around 6549 eV was observed in the final slag (Fig. 6). As shown in Fig. 6 and in the results of the linear combination fit of sulfur shown in Fig. 4, neither MnS nor MnSO_4 were identified in the initial and final slags. Hence, we discuss the relationships between manganese oxide and the X-ray energy of the absorption energy. The absorption K edge of manganese (oxides) other than MnS and MnSO_4 shifted to a lower energy with decreasing oxidation state (Fig. 7). The absorption edge of the carbonated steel slag also shifted to 6544.4 eV from 6549.8 eV after the adsorption of hydrogen sulfide. Therefore, the absorption edge shift observed in the final slag implied that the manganese oxide in the carbonated steel slag was reduced to divalent by the hydrogen sulfide.

During the adsorption experiments, the Eh values of the solution ranged

from -28 to + 46 mV, and the pH ranged from 7.6 to 7.9 for an initial concentration of 10 mg L⁻¹ and -104 to -64 mV and pH 7.8 to 8.0 for 100 mg L⁻¹. The Eh–pH diagram of manganese is shown in Fig. 8, and the range of these adsorption experiment conditions is also shown as a gray-filled area. According to this thermodynamic calculation, divalent manganese (Mn²⁺) is the most stable species under these adsorption experiment conditions. Hence, it is reasonable to suggest that the manganese oxide in the carbonated steel slag was reduced by hydrogen sulfide coupling with the oxidation of hydrogen sulfide.

Conclusion

The adsorption and oxidation behavior of hydrogen sulfide on carbonated steel slag were revealed in this study. Hydrogen sulfide was adsorbed onto the carbonated steel slag with a 7.5 mg g⁻¹ adsorption maximum. The hydrogen sulfide was removed by two processes: (1) the formation of the pyrite and (2) oxidation to sulfur coupled with the reduction of manganese oxide on the carbonated steel slag.

Acknowledgements

Special thanks are given to Kobe Steel LTD and Shinko Slag Co. Ltd., especially Takeshi YAMASHITA and Hiroaki MATSUMOTO for their strong

support.

XAFS analyses at the SR Center, Ritsumeikan University, and the Kyushu Synchrotron Light Research Center were partially carried out under the approval of the open advanced research facility initiative (R1224, R1225 and R1244) and the trial program (111106PT), respectively.

This study was conducted by joint research between Kobe University and KOBELCO Research Institute INC.

This manuscript was critically edited by a native English speaker, Dr. Lawrence M. Liao of the Graduate School of Biosphere Science at Hiroshima University.

References

- [1] Nippon Slag Association, <http://www.slg.jp/statistics/jyukyu/index.html>
(accessed February 12th 2013).
- [2] H. Motz, J. Geiseler, Products of steel slags an opportunity to save
natural resources, Waste Manage. 21 (2001) 285-293.
- [3] C. Barca, C. Gérente, D. Meyer, F. Chazarenc, Y. Andrés, Phosphate
removal from synthetic and real wastewater using steel slags produced
in Europe, Water Res. 46 (2012) 2376-2384.
- [4] E. H. Kim, D. W. Lee, H. K. Hwang, S. Yim, Recovery of phosphates from

wastewater using converter slag: kinetics analysis of a completely mixed phosphorus crystallization process, *Chemosphere* 63 (2006) 192-201.

[5] W. Cha, J. Kim, H. Choi, Evaluation of steel slag for organic and inorganic removals in soil aquifer treatment, *Water Res.* 40 (2006) 1034-1042.

[6] S. Asaoka, T. Yamamoto, Blast furnace slag can effectively remediate coastal marine sediments affected by organic enrichment, *Mar. Poll. Bull.* 60 (2010) 573-578.

[7] A. Hayashi, T. Watanabe, R. Kaneko, A. Takano, K. Takahashi, Y. Miyata, S. Matsuo, T. Yamamoto, R. Inoue, T. Ariyama, Decrease of sulfide in enclosed coastal sea by using steelmaking slag, *Tetsu-to-Hagané* 98 (2012) 207-214 (in Japanese with English abstract).

[8] R. N. Yong, V. R. Ouhadi, Experimental study on instability of bases on natural and lime/cement-stabilized clayey soils, *App. Clay Sci.* 35 (2007) 238-249.

[9] C. Shi, R. L. Day, Pozzolanic reaction in the presence of chemical activators Part II. Reaction products and mechanism, *Cement*

Concrete Res. 30 (2000) 607-613.

- [10] K. R. Hinga, Co-occurrence of dinoflagellate blooms and high pH in marine enclosures, Mar. Ecol. Prog. Ser. 86, (1992) 181-187.
- [11] M. Taraldsvik, S. M. Myklestad, The effect of pH on growth rate, biochemical composition and extracellular carbohydrate production of the marine diatom *Skeletonema costatum*, Europ J. Phycol. 35 (2000) 189-194.
- [12] S. Asaoka, T. Yamamoto, K. Yamamoto, A preliminary study of coastal sediment amendment with granulated coal ash: Nutrient elution test and experiment on *Skeletonema costatum* growth, J. Japan Soc. Water Environ. 31 (2008) 455-462 (in Japanese with English abstract).
- [13] O. Miki, T. Kato, N. Tsutsumi, Phosphorous release control from coastal sediments by carbonated steelmaking slag, J. Japan Soc. Water Environ. 32 (2009) 33-39 (in Japanese with English abstract).
- [14] F. Puertas, M. Palacios, T. Vázquez, Carbonation process of alkali-activated slag mortars, J. Mater. Sci. 41 (2006) 3071-3082.
- [15] W. J. J. Huijgen, G. J. Witkamp, R. N. J. Comans, Mineral CO₂ sequestration by steel slag carbonation, Environ. Sci. Technol. 39

(2005) 9676-9682.

- [16] A. Hayashi, S. Asaoka, T. Watanabe, R. Kaneko, K. Takahashi, Y. Miyata, K. H. Kim, T. Yamamoto, R. Inoue, T. Ariyama, Mechanism of suppression of sulfide ion in seawater using steelmaking slag, *Tetsu-to-Hagané* 98 (2012) 618-625 (in Japanese with English abstract).
- [17] K. H. Kim, S. Asaoka, T. Yamamoto, S. Hayakawa, K. Takeda, M. Katayama, T. Onoue, Mechanisms of hydrogen sulfide removal with steel making slag , *Environ. Sci. Technol.* 46 (2012) 10169-10174.
- [18] S. Asaoka, T. Yamamoto, Y. Takahashi, H. Yamamoto, K. H. Kim, K. Orimoto, Development of an on-site simplified determination method for hydrogen sulfide in marine sediment pore water using a shipboard ion electrode with consideration of hydrogen sulfide oxidation rate, *Interdisciplinary Studies Environ. Chem. – Environ. Poll. Ecotoxicol.* 6 (2012) 345-352.
- [19] E.G. Affonso, V. L. P. Polez, C. F. Corrêa, A. F. Mazon, M. R. R. Araújo, G. Moraes, F. T. Rantin, Physiological responses to sulfide toxicity by the air-breathing catfish, *Hoplosternum littorale* (Siluriformes,

- Callichthyidae), *Comparative Biochem. Physiol.*, C 139 (2004) 251-257.
- [20] K. Marumo, M. Yokota, Review on aoshio and biological effects of hydrogen sulfide. *Rep. Mar. Ecol. Res. Inst.* 15 (2012) 23-40. in Japanese.
- [21] ISO 2597-2, Iron ores -Determination of total iron content- Part 2: Titrimetric methods after titanium(III) chloride reduction, International Organization for Standardization, Geneva, Switzerland, 2008.
- [22] JISR9011, Test methods of lime, Japanese Industrial Standards Committee, Tokyo, Japan, 2006
- [23] JIS-K-0058-2, Test methods of content determination, Japanese Industrial Standards Committee, Tokyo, Japan, 2005
- [24] L. S. Clesceri, A. E. Greenberg, A. D. Eaton (eds), Standard method for the examination of water and wastewater 20th edition, Part 3000 to Part 6000, American Public Health Association, American Water Works Association, Water Environment Federation, Washington D. C., 1999.
- [25] L. Backnaes, J. Stelling, H. Behrens, J. Goettlicher, S. Mangold, O. Verheijen, R. G. C. Beerkens, J. Deubener, Dissolution mechanisms of tetravalent sulphur in silicate melts: evidences from sulphur K edge

- XANES studies on glasses, J. American Ceramic Soc. 91 (2008) 721-727.
- [26] S. Y. Liu, J. Gao, Y. J. Yang, Y. C. Yang, Z. X. Ye, Adsorption intrinsic kinetics and isotherms of lead ions on steel slag, J. Hazard. Mater. 173 (2010) 558-562.
- [27] J. Xiong, Z. He, Q. Mahmood, D. Liu, X. Yang, E. Islam, Phosphate removal from solution using steel slag through magnetic separation, J. Hazard. Mater. 152 (2008) 211-215.
- [28] C. Oh, S. Rhee, M. Oh, J. Park, J., Removal characteristics of As(III) and As(V) from acidic aqueous solution by steel making slag, J. Hazard. Mater. (2012) 147-155.
- [29] S. Asaoka, T. Yamamoto, S. Hayakawa, Removal of hydrogen sulfide using granulated coal ash, J. Japan Soc. Water Environ. 32 (2009) 363-368 (in Japanese with English abstract).
- [30] S. Asaoka, T. Yamamoto, S. Kondo, S. Hayakawa, Removal of hydrogen sulfide using crushed oyster shell from pore water to remediate organically enriched coastal marine sediments, Biores. Technol. 100 (2009) 4127-4132.

- [31] Y. Onganer, Ç. Temur, Adsorption dynamics of Fe(III) from aqueous solutions onto activated carbon, *J. Colloid Interf. Sci.* 205 (1998) 241-244.
- [32] Y. S. Ho, A. E. Ofomaja, Pseudo-second-order model for lead ion sorption from aqueous solutions onto palm kernel fiber, *J. Hazard. Mater.* B129 (2006) 137-142.
- [33] M. Y. Chang, R. S. Juang, Adsorption of tannic acid, humic acid, and dyes from water using the composite of chitosan and activated clay, *J. Colloid Interf. Sci.* 278 (2004) 18-25.
- [34] S. Asaoka, S. Hayakawa, K. H. Kim, K. Takeda, M. Katayama, T. Yamamoto, Combined adsorption and oxidation mechanisms of hydrogen sulfide on granulated coal ash, *J. Colloid Interf. Sci.* 377 (2012) 284-290.

Figure captions

Fig. 1 SEM images and chemical composition of the small particles.

Fig. 2 Adsorption kinetics of hydrogen sulfide onto the carbonated steel slag

●: Initial concentration 10 mg L⁻¹; ○: Initial concentration 100 mg L⁻¹

Error bars show standard deviation in triplicates.

Fig. 3 Adsorption kinetics of hydrogen sulfide onto the carbonated steel slag described by the pseudo-first-order equation

●: Initial concentration 10 mg L⁻¹; ○: Initial concentration 100 mg L⁻¹

Fig. 4 The sulfur K edge XANES spectra of the final slag and the yellow-colored hydrogen sulfide solution

The pyrite and sulfur standard are also given. The final slag is hydrogen-sulfide-adsorbed carbonated steel slag. The dotted lines are curve-fitting results using the standard spectrum.

Fig. 5 The iron K edge XANES spectra of the initial and final slags and iron standards

The initial slag and final slag are carbonated steel slag without and with the adsorption of hydrogen sulfide, respectively. The dotted lines are curve-fitting results using the standard spectrum.

Fig. 6 The manganese K edge XANES spectra of the initial and final slags and manganese standards

The initial slag and final slag are carbonated steel slag without and with the adsorption of hydrogen sulfide, respectively.

Fig. 7 Relationship between the valence of the manganese (oxide) and the X-ray energy of the absorption edge

Fig. 8 Eh–pH diagram of manganese.

The shaded area represents the adsorption experiment conditions.

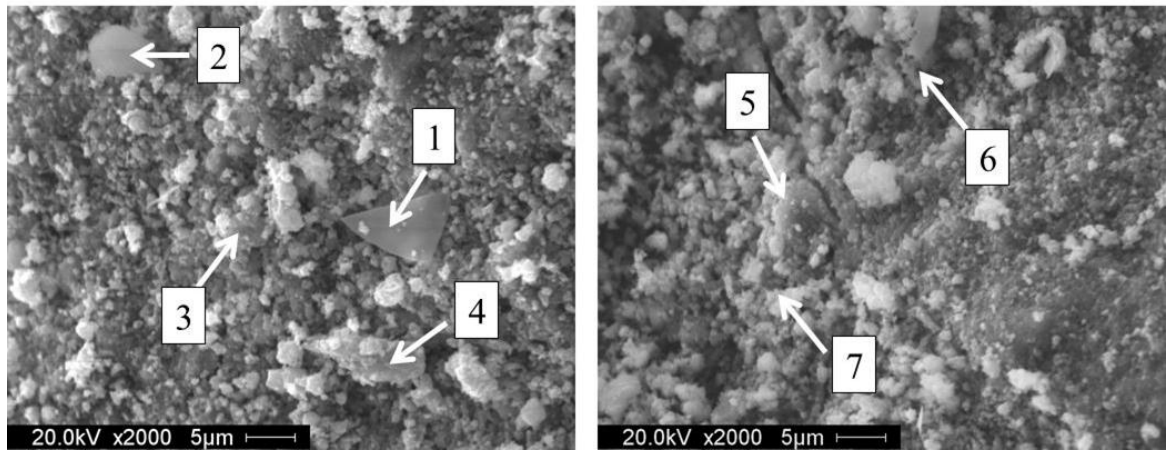


Fig. 1

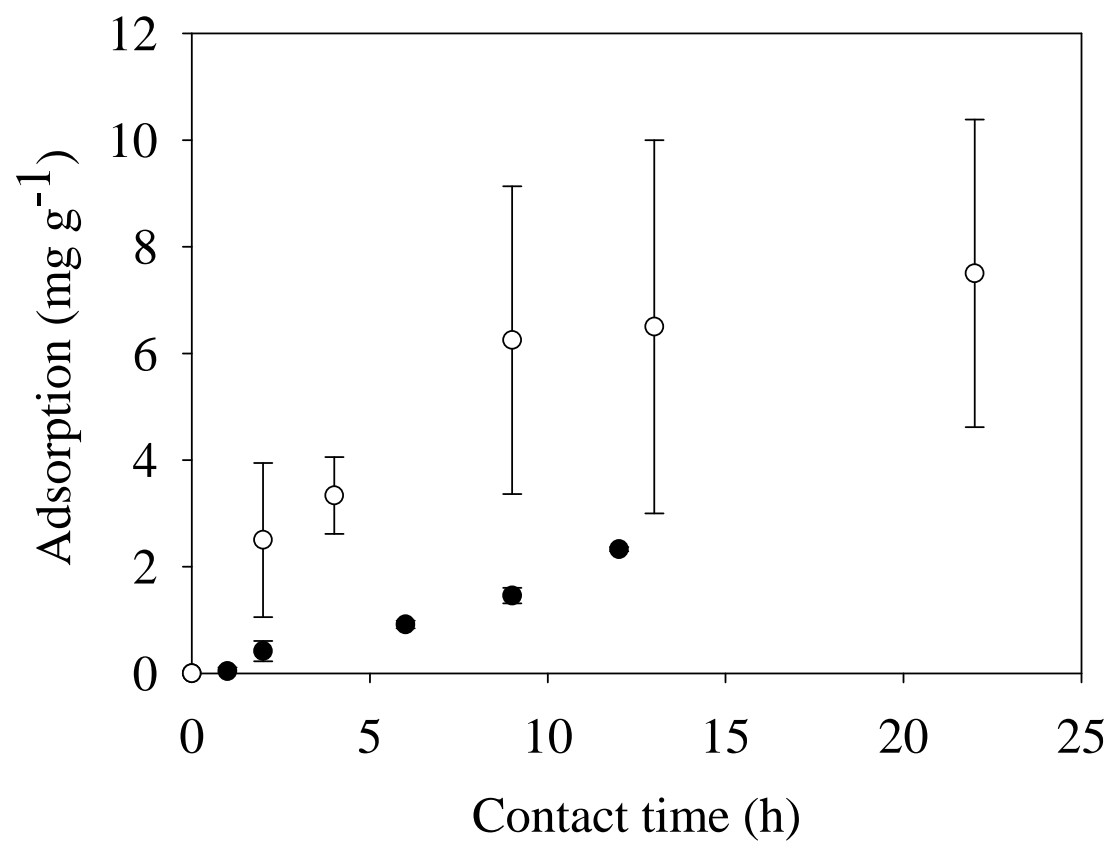


Fig. 2

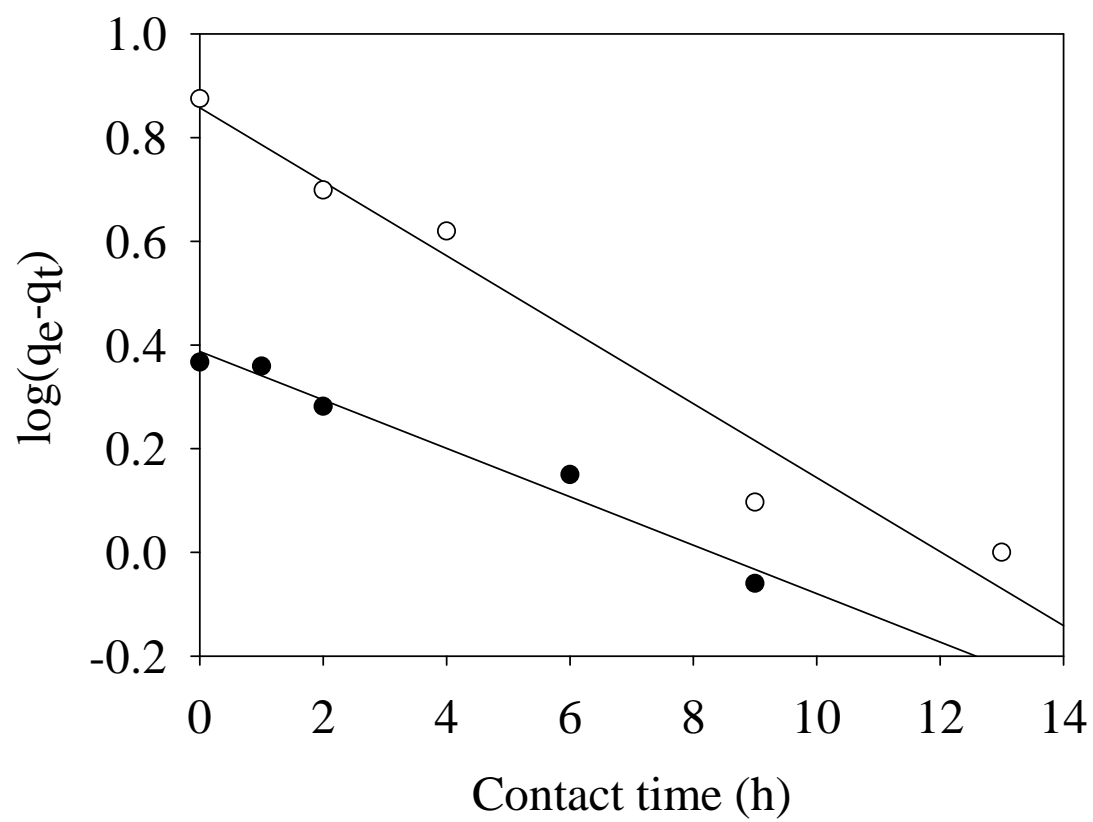


Fig. 3

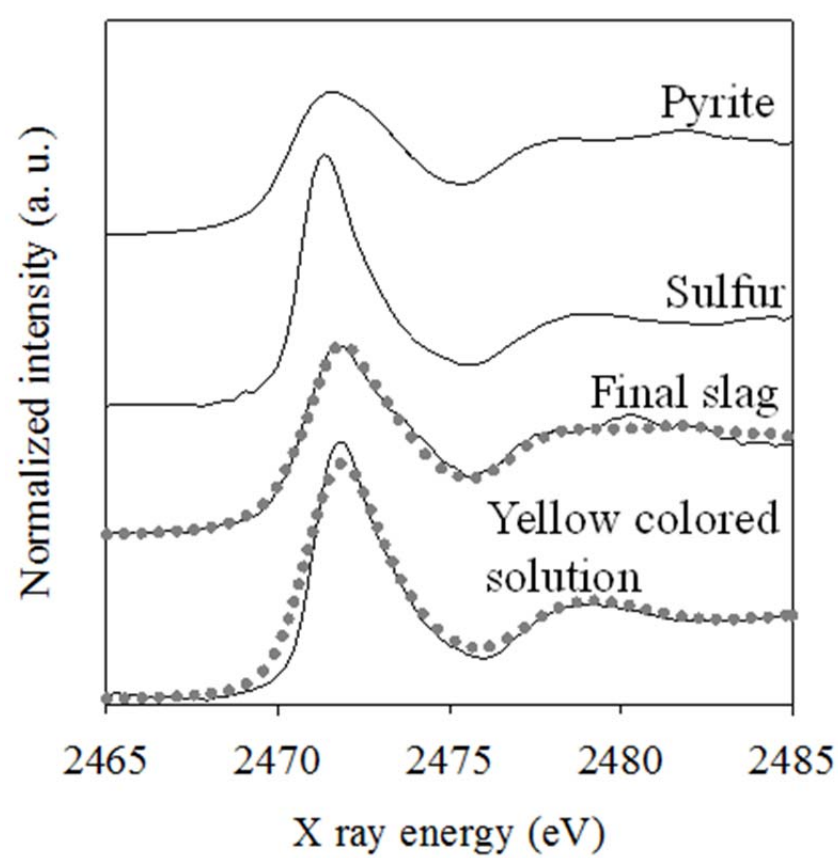


Fig. 4

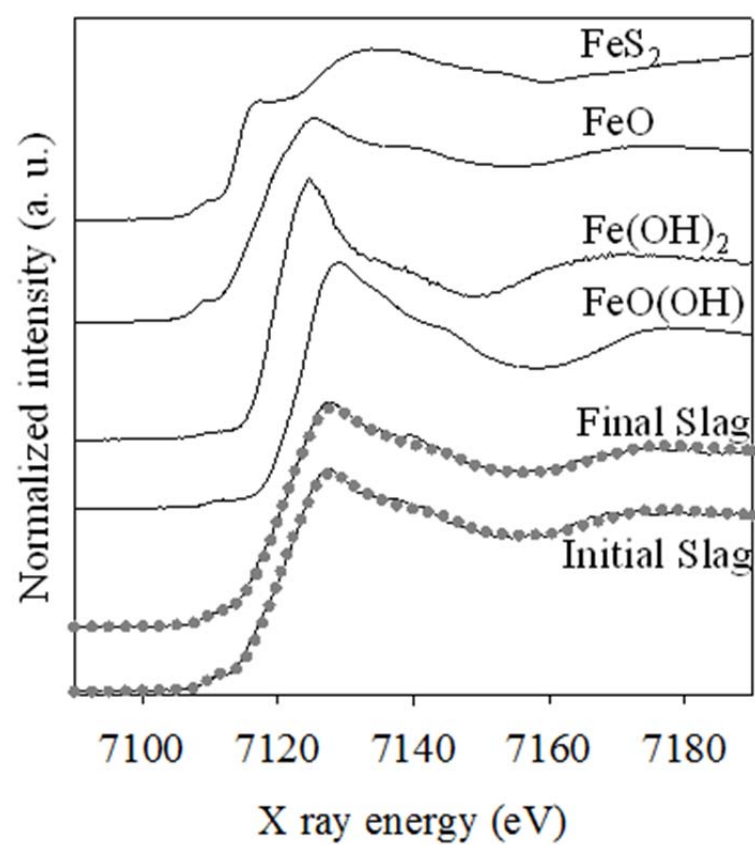


Fig.5

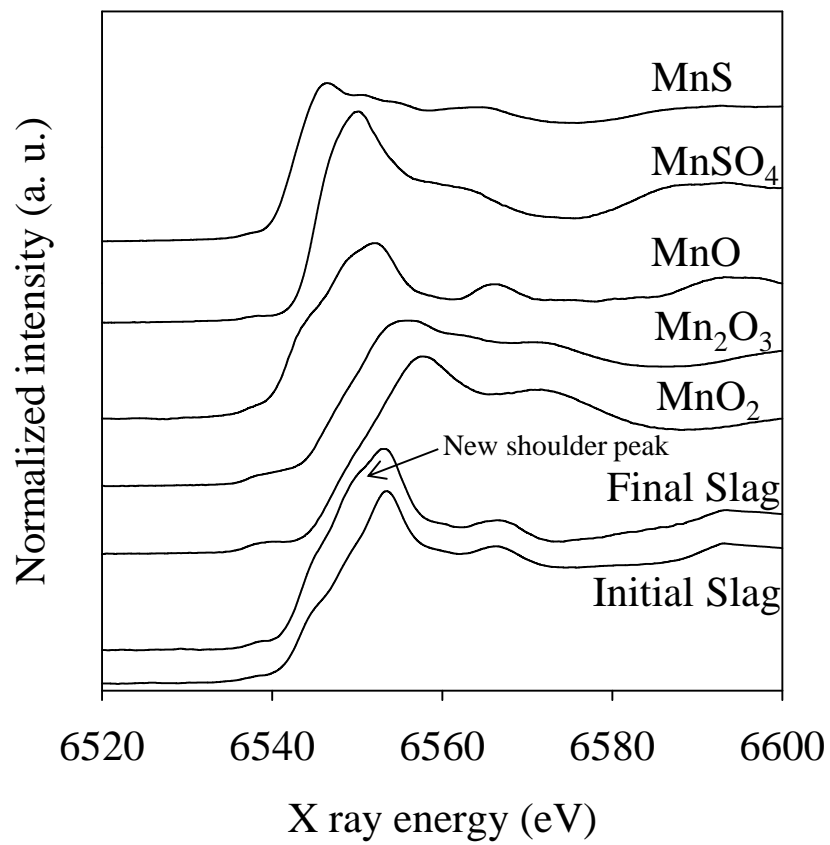


Fig. 6

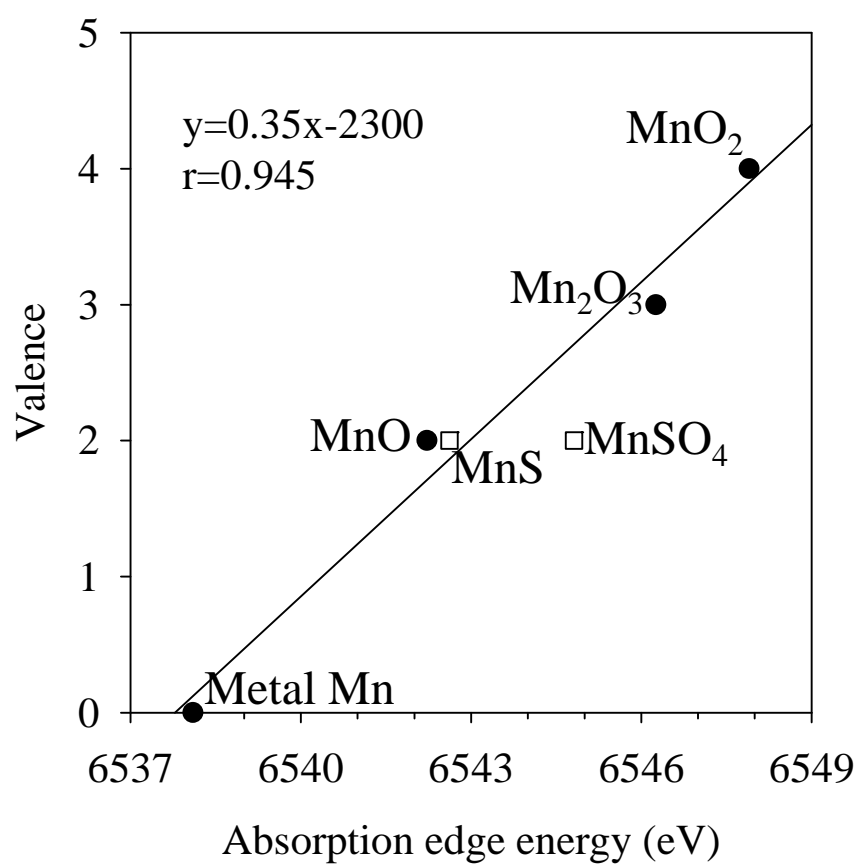


Fig. 7

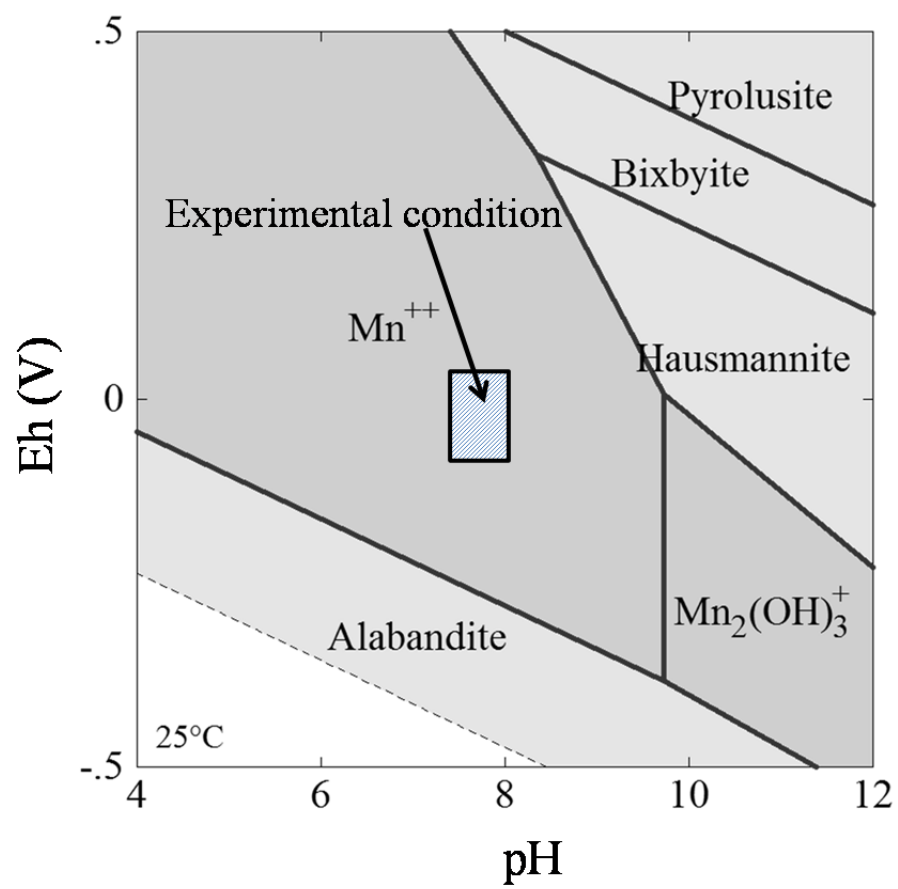


Fig. 8

Tables

Table 1 Percent composition of the carbonated steel slag used in this study

Compounds	(%)	Analytical Methods
CaCO ₃	29.9	Titration
Total-Fe	18.8	Titration
CaO	18.7	XRF
SiO ₂	9.5	XRF
MgO	4.4	XRF
Al ₂ O ₃	3.2	XRF
MnO	2.8	XRF
P ₂ O ₅	1.1	XRF
S	0.1	Carbon/Sulfur analyzer
Others	11.5	-

Table 2 Concentrations of environmentally regulated substances in the carbonated steel slag used in this study

Target	Concentration (mg kg ⁻¹)	Criterion (mg kg ⁻¹)	Analytical Methods
Total Hg	<0.1	<15	CV-AAS ¹⁾
Cd	<5	<150	ICP-MS
CN	<1	<50	AP ²⁾
Pb	<5	<150	ICP-MS
Cr(+VI)	<5	<250	ICP-AES
As	<5	<150	HG-AAS ³⁾
Se	<5	<150	HG-AAS
F	77	<4000	AP
B	39	<4000	ICP-AES

1) Cold Vapor Atomic Adsorption Spectrometry; 2) Adsorption Photometry; 3) Hydride Generation Atomic Adsorption Spectrometry

Table 3 Concentrations of environmentally regulated substances dissolved from the carbonated steel slag used in this study

Target	Concentration (mg L ⁻¹)*	Criterion (mg L ⁻¹)	Analytical Methods
Alkyl Hg	<0.0005	ND	GC
Total Hg	<0.0005	<0.0005	CV-AAS ¹⁾
Cd	<0.001	<0.01	ICP-MS
Pb	<0.005	<0.01	ICP-MS
Organic P	<0.1	ND	GC
Cr(+VI)	<0.01	<0.05	ICP-AES
As	<0.002	<0.01	HG-AAS ²⁾
Total CN	<0.1	ND	AP ³⁾
PCB	<0.0005	ND	GC
Trichloroethylene	<0.002	<0.03	HS-GC-MS ⁴⁾
Tetrachloroethylene	<0.0005	<0.01	HS-GC-MS
Dichloromethane	<0.002	<0.02	HS-GC-MS
Carbon tetrachloride	<0.0002	<0.002	HS-GC-MS
1, 2-dichloroethane	<0.0004	<0.004	HS-GC-MS
1, 1-dichloroethylene	<0.002	<0.02	HS-GC-MS
cis-1, 2-dichloroethylene	<0.004	<0.04	HS-GC-MS
1, 1, 1-trichloroethane	<0.001	<1	HS-GC-MS
1, 1, 2-trichloroethane	<0.0006	<0.006	HS-GC-MS
1, 3-dichloropropene	<0.0002	<0.002	HS-GC-MS
Thiuram	<0.0006	<0.006	SPE-HPLC ⁵⁾
Simazine	<0.0003	<0.003	SPE-GC-MS ⁶⁾
Thiobencarb	<0.002	<0.02	SPE-GC-MS
Benzene	<0.001	<0.01	HS-GC-MS
Se	<0.002	<0.01	H-AAS
F	<0.2	<0.8	AP
B	<0.2	<1	ICP-AES

1) Cold Vapor Atomic Adsorption Spectrometry; 2) Hydride Generation Atomic Absorption Spectrometry; 3) Absorption Photometry; 4) Head space Gas chromatography and Mass spectrometry; 5) Solid Phase Extraction High Performance Liquid Chromatography; 6) Solid Phase Extraction Gas chromatography

*Solid and liquid ratio is 10 w/v.

Table 4 Chemical composition of the small particles in Fig. 1 (wt.%)

Elements	Particle 1	Particle 2	Particle 3	Particle 4	Particle 5	Particle 6	Particle 7
C	17.6	12.7	14.3	13.1	9.2	15.7	17.0
O	38.3	33.5	30.8	34.9	25.6	42.3	44.2
Na	-	-	-	1.0	-	-	-
Mg	1.4	-	1.6	0.6	1.4	0.8	1.2
Al	4.1	0.8	2.9	1.0	1.0	4.8	1.0
Si	8.4	2.3	6.8	2.7	8.1	8.3	5.4
Ca	26.8	50.7	26.8	44.6	46.3	24.3	26.9
Ti	-	-	2.0	-	-	-	-
Mn	0.8	-	-	-	1.7	-	-
Fe	2.3	-	12.3	-	6.7	1.9	2.6
Cu	-	-	-	2.2	-	-	-
Zn	-	-	2.6	-	-	2.0	1.7

-: not detected

Table 5 Correlation coefficient for the linear regression of each kinetic equation

Equation	Initial concentration (mg L ⁻¹)	
	10	100
Pseudo first order	0.989	0.982
Pseudo second order	0.970	0.216
Intraparticle diffusion	0.905	0.981